

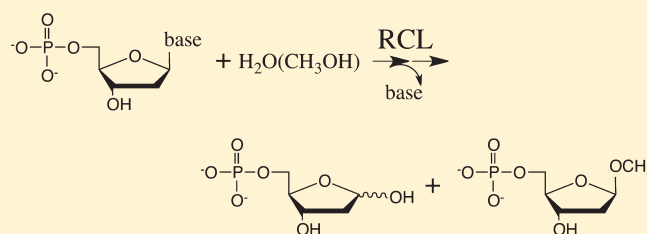
# RCL Hydrolyzes 2'-Deoxyribonucleoside 5'-Monophosphate via Formation of a Reaction Intermediate

Kiran Doddapaneni,<sup>†</sup> Walter Zahurancik,<sup>†</sup> Adam Haushalter,<sup>†</sup> Chunhua Yuan,<sup>‡</sup> Jane Jackman,<sup>†</sup> and Zhengrong Wu<sup>\*,†</sup>

<sup>†</sup>Biochemistry Department, Ohio State University, Columbus, Ohio 43210, United States

<sup>‡</sup>Campus Chemical Instrument Center, Ohio State University, Columbus, Ohio 43210, United States

**ABSTRACT:** RCL is an enzyme that catalyzes the *N*-glycosidic bond cleavage of purine 2'-deoxyribonucleoside 5'-monophosphates. Recently, the structures of both free wild type and GMP-bound mutant complex have been determined by multi-dimensional NMR, revealing a doubly wound  $\alpha/\beta$  protein existing in a symmetric homodimer. In this work, we investigated the catalytic mechanism by rational site-directed mutagenesis, steady-state and pre-steady-state kinetics, ITC binding analysis, methanolysis, and NMR study. First, we provide kinetic evidence in support of the structural studies that RCL functions in a dimeric form, with an apparent dissociation constant around 0.5  $\mu$ M in the presence of substrate dGMP. Second, among the eight residues under investigation, the highly conserved Glu93 is absolutely critical and Tyr13 is also important likely contributing to the chemical step, whereas Ser117 from the neighboring subunit and Ser87 could be the key residues for the phosphate group recognition. Lastly, we demonstrate by methanolysis study that the catalytic reaction proceeds via the formation of a reaction intermediate, which is subsequently hydrolyzed by solvent nucleophile resulting in the formation of normal product deoxyribose monophosphate (dRSP) or methylated-dRSP. In conclusion, the current study provides mechanistic insights into a new class of nucleotide hydrolase, which resembles nucleoside 2'-deoxyribosyltransferases structurally and functionally but also possesses clear distinction.



RCL (responsive to c-Myc), a purine 2'-deoxyribonucleoside 5'-monophosphate *N*-glycosidase, represents a novel class of nucleotide hydrolases that catalyze the cleavage of the *N*-glycosidic bond of 2'-deoxyribonucleoside 5'-monophosphates, preferentially on dGMP, resulting in deoxyribose 5'-phosphate (dRSP) and the corresponding nucleobase.<sup>1</sup> The biological role(s) of RCL is currently unclear, and it has been suggested to be important for the fate of cell growth and cell proliferation.<sup>2–5</sup> In response to c-Myc, significant upregulation of RCL has been noticed in selective cancers such as breast cancer,<sup>2,6</sup> prostate cancer,<sup>7</sup> lymphoma,<sup>2,8–10</sup> and glioblastoma.<sup>1</sup> The enzyme has been related to the nucleoside deoxyribosyltransferase (NDT) on the basis of sequence alignment.<sup>1</sup> Recent structural studies on the apo-RCL<sup>11</sup> and GMP-bound D69A mutant complex<sup>12</sup> revealed a symmetric homodimer with each subunit comprising a five-stranded parallel  $\beta$ -sheet sandwiched between five  $\alpha$ -helices, a doubly wound  $\alpha/\beta$  architecture resembling NDT. The latter—an essential enzyme in the nucleoside salvage pathway of certain microorganisms—catalyzes the transfer of a deoxyribose moiety from a donor deoxyribonucleoside to an acceptor base.<sup>13</sup> Its ping-pong-bi-bi mechanism invokes the formation of a covalent enzyme–deoxyribosyl intermediate,<sup>14,15</sup> which results in the retention of anomeric stereochemical configuration of the deoxyribose in the final product.<sup>15</sup> In the absence of an acceptor base, the intermediate can be slowly hydrolyzed.<sup>16</sup> Furthermore, a conserved glutamyl residue has been identified as the nucleophile for

the bond cleavage, and its mutation significantly decreases the NTD's hydrolase activity. Mutation of other residues including the conserved Tyr7, by contrast, appeared to be tolerable for such activity.<sup>16</sup>

While sharing a similar topology as well as the conserved Tyr13, Asp69, and Glu93 in the active site with NDTs, RCL clearly lacks the structural features needed for the transferase activity, for example, the structured C-terminal tail reaching to the active site.<sup>11</sup> Furthermore, the enzyme differs from the transferases by possessing a distinct phosphate binding pocket, comprising residues likely from both subunits in a dimer, including Ser17, Arg19, Ser87, and Ser117<sup>#</sup> (# denotes residues from neighboring unit).<sup>11,12</sup> More importantly, in an early study by Kaminski and co-workers, it was reported that the enzymatic activity was unaffected in the alanine mutant of Glu93—equivalent to the nucleophilic glutamyl residue in NDTs—and the hydrolysis reaction appeared to be irreversible, leading to a speculation that RCL is mechanistically different from NDTs.<sup>1,17</sup>

Toward a better understanding of the catalytic mechanism of this novel enzyme, in this work we performed a study using a multifaceted approach, including rational site-directed mutagenesis, steady-state and pre-steady-state kinetics, ITC assay,

**Received:** November 1, 2010

**Revised:** April 20, 2011

**Published:** April 21, 2011

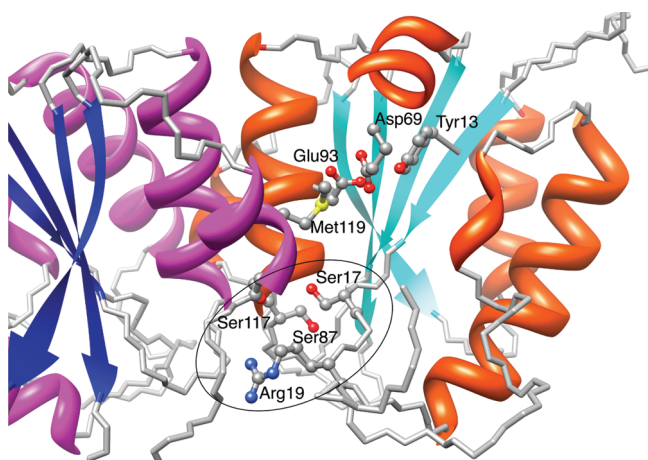


**Figure 1.** Active site residues that have been mutated (PDB code 2KHZ). Helices from two subunits in RCL dimer are colored in orange and magenta, respectively. Residues proposed to be important for phosphate group binding are encircled.

methanolysis, and NMR study, intended to address three important issues: (1) What is the relationship between RCL oligomeric state and its catalytic activity? (2) Do the residues implicated in functional roles on the basis of NMR structures really contribute substantially to the chemistry and/or substrate binding? These include the aforementioned potential catalytic and phosphate binding residues illustrated in Figure 1. (3) Does there exist an intermediate in the reaction pathway in analogy to the one observed in NDTs<sup>14</sup> or, alternatively, in reminiscent of nucleoside hydrolases,<sup>18,19</sup> an enzyme-activated water molecule serving as a nucleophile to directly attack the C1' of dGMP with the concomitant departure of the nucleobase? Taken together, our results strongly suggested that (i) the dimeric rather than the monomeric RCL is the catalytically active form; (ii) the conserved Glu93 is likely the nucleophile and the Tyr13 is another catalytically important residue for the chemistry, whereas Ser87 and Ser117<sup>#</sup> are important for the phosphate group recognition; and (iii) RCL indeed catalyzes the dGMP hydrolysis via a rate-limiting step of formation of a reaction intermediate, which can be reversibly hydrolyzed by solvent molecules.

## MATERIALS AND METHODS

### Mutagenesis and Purification of Rat RCL and the Mutants.

Selected amino acids were replaced by site-directed mutagenesis of rat RCL gene using QuickChange mutagenesis kit (Stratagene). It is noteworthy that at least two nucleotides per codon were changed to minimize potential translational misincorporation. The desired nucleotide sequences were confirmed by sequencing, and each corresponding mutant enzyme was further verified by mass spectrometry. The procedure of protein expression and purification has been described in detail previously.<sup>11</sup> Extra caution has been taken to ensure negligible cross-contamination particularly from trace amount of WT protein. Briefly, a new Ni column was packed for each mutant, and the size-exclusion column was extensively washed. More importantly, a catalytically impaired double mutant E93A/Y13A was purified serving as a control immediately before the purification of each single mutant protein. These mutant proteins were confirmed to adopt WT-like tertiary fold by <sup>1</sup>H NMR. Protein

concentration was measured spectrophotometrically at 280 nm using an extinction coefficient,  $\epsilon_{280}$ , of  $21\,555\text{ M}^{-1}\text{ cm}^{-1}$ .

**Synthesis of dGMP.** <sup>32</sup>P-dGMP was enzymatically converted from [ $\alpha$ -<sup>32</sup>P]-dGTP (Perkin-Elmer) using *mutT* nucleoside triphosphatase of *E. coli* purified according to the method described by Bhatnagar et al.<sup>20</sup> The total reaction mixture was separated by thin layer chromatography (Silica gel 60 F<sub>254</sub>, EMD chemicals) with a solvent mixture of *n*-propanol/ $\text{NH}_4\text{OH}/\text{H}_2\text{O}$  (55/35/10, v/v). The dGMP band was scraped, and the product was extracted with 1 mL of water for 2 h, followed by lyophilization twice to remove any organic solvent. The final recovery rate of <sup>32</sup>P-dGMP was greater than 95%. The rate of hydrolysis of this labeled dGMP is consistent with that of the commercial dGMP using a coupled enzymatic assay detailed previously.<sup>1</sup>

**Kinetic Analysis.** Hydrolysis activity of RCL was determined by directly monitoring the liberation of <sup>32</sup>P-deoxyribose 5'-monophosphate (dR5P) from the substrate <sup>32</sup>P-dGMP. Unless stated otherwise, the standard reaction mixture consists of 50 mM Tris acetate (pH 6.0), variable concentrations of unlabeled-dGMP along with 10 000 cpm of the <sup>32</sup>P-dGMP in a final reaction volume of 20  $\mu\text{L}$ . All reactions were carried out at 37 °C. Aliquots of the reaction mixture were collected at variable time points, and the reaction was quenched by either heat deactivation or 2 M formic acid. 2  $\mu\text{L}$  of the resulting sample was spotted on a PEI cellulose TLC plate (EMD Chemicals) and resolved in a solvent system comprising 0.5 M potassium phosphate buffer (pH 6.3)/MeOH (80/20, v/v). The plates were visualized with a Typhoon phosphorimager and quantified using IMAGE-QUANT software (GE Healthsciences). In all reactions, the steady-state condition was met by allowing 10% or less of substrate conversion. Initial velocities at each substrate concentration were determined in duplicate data sets and fitted to the Michaelis–Menten equation through nonlinear regression using Kaleida/nospace graph version 4.03. Control assays, in the absence of enzyme, were routinely included. Any nonenzyme-assisted degradation of the substrate, if any, was subtracted from the reaction.

Dimer/monomer equilibrium of RCL was investigated by measuring the specific enzymatic activity as a function of protein concentration, ranging from 0.25 to 100  $\mu\text{M}$ . Assuming only the dimer form of the enzyme contributes to the observed activity, the apparent dissociation constant ( $K_d$ ) was obtained by fitting the above data to the equation:  $V_{\text{obs}} = V_d([E]_t - [M])/[E]_t$ , where  $V_d$  is the maximum specific activity achieved when all enzyme molecules are in an active dimeric form,  $V_{\text{obs}}$  the observed specific activity,  $[E]_t$  the total RCL protomer concentration, and  $[M]$  the concentration of the monomeric form of RCL, which can be substituted with  $[M] = 0.5[-K_d/2 + (K_d^2/4 + 2K_d[E]_t)^{0.5}]$  according to the equilibrium condition ( $K_d = 2[M]^2/([E]_t - [M])$ ).<sup>21</sup> To establish the maximal first-order rate of RCL-catalyzed dGMP hydrolysis (which, as described in the text, is likely to reflect the chemical step of formation of the reaction intermediate), single turnover experiments were performed on both WT and Y13F RCL. Reactions were made pseudo-first-order by using at least 5-fold excess of enzyme in the reactions relative to substrate dGMP (50  $\mu\text{M}$ ). Formation of the product dR5P was measured as a function of reaction time using the same assay described above for steady-state kinetic analysis, except that aliquots of reaction mixture at different time points were immediately quenched by using 2 M formic acid. Compared to heat deactivation, only the WT single turnover result exhibited a notable difference by  $\sim 20\%$ , while for the much slower reaction

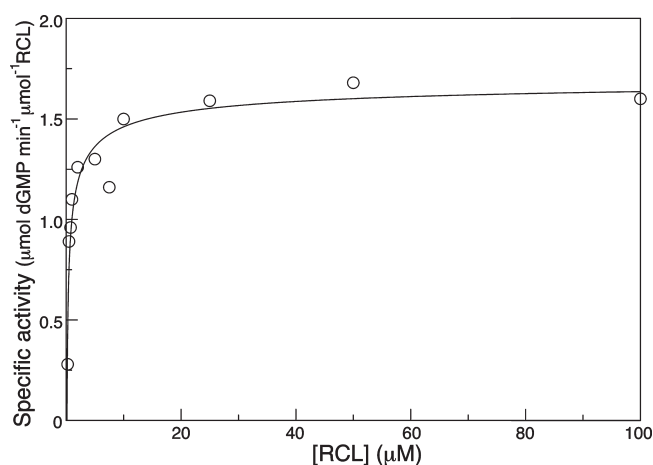


**Figure 2.** Specific activity of RCL as a function of protein concentration in the presence of a constant 1.0 mM dGMP.

by Y13F, these two methods did not make any significant difference. The data were fitted to the first-order rate equation  $[dRSP] = [dRSP]_{\infty}(1 - \exp(-k_{\text{obs}}t))$  to determine the pseudo-first-order rate constant,  $k_{\text{obs}}$ . To ensure that the measured maximal rate constant for hydrolysis ( $k_{\text{chem}}$ ) was enzyme concentration independent,  $k_{\text{obs}}$  was determined in two assays with different high concentrations of enzyme.

**Isothermal Titration Calorimetry.** ITC experiments were carried out by using a VP-ITC calorimeter (MicroCal, Northampton, MA). Wild type and mutant proteins were dialyzed extensively against the ITC buffer [25 mM phosphate (pH 6.5), 25 mM NaCl, 2 mM  $\beta$ -mercaptoethanol]. GMP solution (10 mM at 5  $\mu$ L increments) prepared using the same buffer was titrated into 1.4 mL of 250  $\mu$ M wild type RCL or the mutant proteins at a higher concentration under 25 °C with an 8 min intertitration delay to achieve a flat baseline. The heat of dilution obtained from injecting the ligand into buffer was subtracted before fitting. Data analysis was performed by using Origin 7.0 (MicroCal) and best-fitted using a single binding-site model.

**Methanolysis Reaction.** Methanolysis of 4 mM dGMP was performed in 25 mM phosphate buffer, pH 6.5, 20% methanol, and 10  $\mu$ M RCL at 37 °C as detailed previously.<sup>19</sup> Briefly, 200  $\mu$ L aliquots of the reaction mixture were extracted at various time points and heated to 100 °C for 5 min to deactivate the enzyme, followed by centrifugation to remove any precipitants. The supernatant was then freeze-dried, and the lyophilized powder was dissolved in 99.9% D<sub>2</sub>O (Isotec). To confirm that formation of the MeO-dRSP is independent of dRSP at the early stage of the hydrolysis reaction, one unit of dRSP-aldolase (SIGMA) was added to the above reaction mixture in the presence of 20% methanol, and samples at different time points up to 5 h were obtained. Analysis of the products was performed by <sup>1</sup>H NMR at 600/800 MHz, 2D <sup>1</sup>H–<sup>13</sup>C HMB, and HSQC.

## RESULTS

**Dimeric RCL Is the Catalytically Active Form.** NMR studies revealed a symmetric homodimer in apo- and GMP-bound RCL structures.<sup>11,12</sup> Given that the active site is postulated to comprise residues from both subunits, it is tempting to assume that only the dimer contributes to the hydrolysis activity. However, the NMR studies were performed at submillimolar concentration,

and RCL reportedly exists mostly in a monomeric form under a protein concentration of 3  $\mu$ M and predominantly dimeric above 30  $\mu$ M.<sup>1</sup> It is thus unclear whether the monomer is catalytically active or even more active than the dimer. Here we provide kinetic evidence in support of the structural results that only the dimeric RCL is catalytically active.

We first carried out steady-state kinetic measurements at 2.0  $\mu$ M RCL using a newly developed <sup>32</sup>P-assay as detailed in the Materials and Methods section. The kinetic parameters  $k_{\text{cat}}$  and  $K_m$  were determined to be  $0.03 \pm 0.002 \text{ s}^{-1}$  and  $89 \pm 34 \text{ } \mu\text{M}$ , respectively, which are in good agreement with those obtained using a more complicated coupled method.<sup>1</sup> When the enzyme concentration was lowered to 0.5  $\mu$ M, those values became  $0.018 \pm 0.002 \text{ s}^{-1}$  and  $79 \pm 30 \text{ } \mu\text{M}$ , respectively. Apparently, there is noticeable change in  $k_{\text{cat}}$  while the magnitude of  $K_m$  is hardly affected by enzyme concentration. We further measured the rate of dGMP hydrolysis under the condition of 1 mM substrate with a series of enzyme concentrations ranging from 0.25 to 100  $\mu$ M (Figure 2). It was found that the specific activity increases with RCL concentration and quickly reaches a plateau at less than 10  $\mu$ M. When fitted as detailed in the Materials and Methods section assuming no activity in the monomeric form, the apparent  $K_d$  of the dimer/monomer equilibrium was estimated to be around 0.5  $\mu$ M, about 1 order of magnitude lower than what was reported for the apoenzyme based on an analytical centrifugation method.<sup>1</sup> Such a discrepancy may be attributed to the presence of dGMP substrate, and our result appears to be in consistent with the kinetic data that RCL's activity becomes independent of the protein concentration when above 2  $\mu$ M.

We then examined the Met119 residue, a dimer interfacial residue in close proximity to the catalytic site of the neighboring subunit. While the exact functional role has yet to be determined, this residue in NDT was proposed to help orient and/or anchor the substrate at the active site. It was found that the M119A of RCL diminished the activity by more than 80-fold with respect to WT (Table 1).

**Glu93 and Tyr13 Are Catalytically Important.** As pointed out earlier, structural-based sequence alignment revealed that the highly conserved Tyr13, Asp69, and Glu93 in the postulated active site coincide with their counterparts in NDTs.<sup>11,12</sup> To evaluate their catalytic roles, these residues were mutated and tested for activity using the <sup>32</sup>P kinetic assay (Table 1). With respect to WT, the single mutant E93A and double mutants E93AY13A and E93AD69A all showed undetectable activity, indicating a more than 10<sup>5</sup>-fold drop in enzyme activity. The observation with E93A is in sharp contrast with the previous report on the same mutant in which only  $K_m$  but not  $k_{\text{cat}}$  was affected.<sup>1,17</sup> While the cause of such discrepancy is unclear, our result appears to be in parallel with similar studies in both NDTs<sup>16</sup> and Blsm,<sup>23</sup> where significantly or completely impaired hydrolytic activity was detected. Y13F mutant exhibits a 280-fold reduction in  $k_{\text{cat}}/K_m$  with a WT-like  $K_m$ , suggesting that the effect of this substitution does not impact overall substrate binding. The marked reduction in activity upon substitution of Tyr13 is surprising, as the equivalent mutation of Y7A in the NDT showed negligible effect on the hydrolysis reaction.<sup>16</sup> It is plausible that this tyrosyl residue may play a different functional role in RCL. Finally, D69A only caused a marginal ~6-fold reduction in  $k_{\text{cat}}$ , a value comparable to the previous report.<sup>12</sup>

To further delineate the catalytic role of Tyr13, single turnover kinetic experiments were performed on both WT and Y13F to



**Table 1. Kinetic Parameters for dGMP Hydrolysis by RCL**

RCL	$k_{\text{cat}} (\times 10^{-2} \text{ s}^{-1})$	$K_{\text{M}} (\mu\text{M})$	$k_{\text{cat}}/K_{\text{M}} (\text{M}^{-1} \text{ s}^{-1})$	fold reduced activity <sup>a</sup>	$k_{\text{chem}}^b (\times 10^{-2} \text{ s}^{-1})$	$K_{\text{D}} (\text{GMP})$
WT	3.0 ± 0.2	89 ± 34	341 ± 60		6.2 ± 0.5	9.7 ± 0.3
Y13F	0.017 ± 0.003	165 ± 33	1.2 ± 0.4	284	0.036 ± 0.003	
E93A	nd <sup>c</sup>	nd			nd	
D69A	0.52 ± 0.03	341 ± 69	15 ± 3	23		
S17A	2.8 ± 0.3	666 ± 198	41 ± 9	8		17 ± 2
R19A	5.8 ± 0.3	372 ± 85	158 ± 29	2		97 ± 2
S87A	0.71 ± 0.06	1193 ± 444	6 ± 2	57		338 ± 6
S117A	0.095 ± 0.004	3607 ± 463	0.3 ± 0.01	1137		847 ± 15
M119A	0.12 ± 0.03	285 ± 33	4.1 ± 0.4	83		

<sup>a</sup> Calculated as  $(k_{\text{cat}}/K_{\text{M,WT}})/(k_{\text{cat}}/K_{\text{M,mut}})$ . <sup>b</sup> Average of single-turnover  $k_{\text{obs}}$  measured at two different high concentrations of each enzyme. <sup>c</sup> Nondetectable.

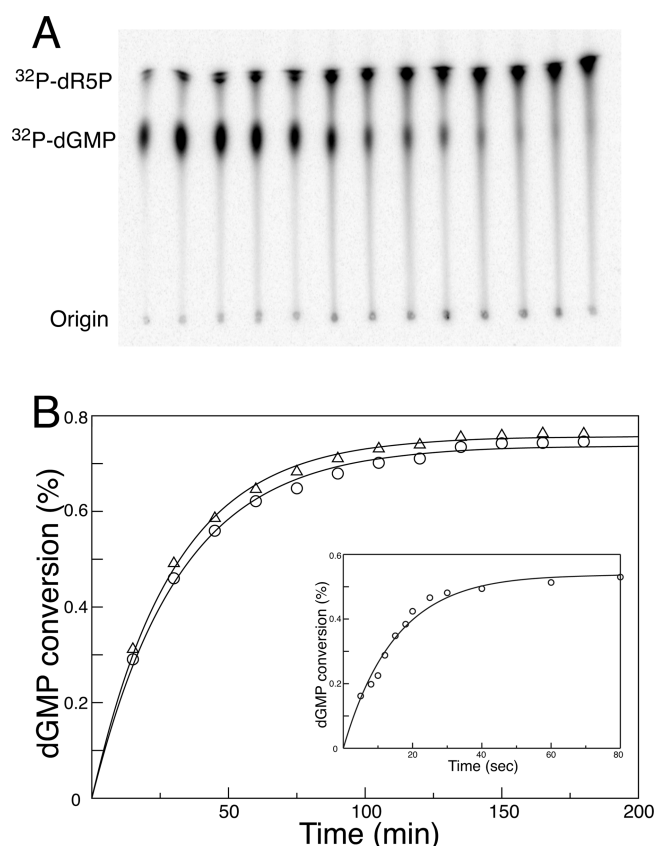
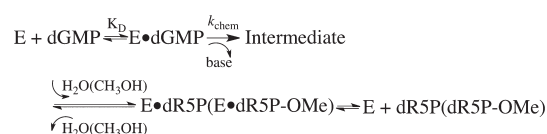


**Figure 3.** Single turnover result for Y13F mutant: (A) Hydrolysis of <sup>32</sup>P-dGMP by monitoring the rate of formation of <sup>32</sup>P-dR5P formation as a function of time. (B) Conversion of dGMP observed in (A) is fitted to first-order rate equation under two different RCL concentrations, 400 μM (○) and 1000 μM (Δ), to yield  $k_{\text{obs}}$  for RCL catalysis. As a comparison, the inset in (B) shows the single turnover result of WT RCL fitted to first-order rate equation.

isolate the individual step of dGMP hydrolysis along the reaction pathway. Time courses of dGMP hydrolysis measured under single turnover conditions (large excess of enzyme relative to substrate) were fitted well by a single-exponential equation to yield the  $k_{\text{obs}}$  (Figure 3). Moreover, at the high enzyme concentrations used for these assays (>400 μM for each enzyme), the measured  $k_{\text{obs}}$  did not show concentration-dependent behavior, indicating that formation of the E•dGMP complex is not

**Scheme 1. Proposed Reaction Pathway Catalyzed by RCL**



rate limiting. Under this condition, the measured  $k_{\text{obs}}$  reflects the rate-determining first-order step for dGMP hydrolysis. Since the single turnover TLC assay does not distinguish between RCL-bound (E•dRSP, see Scheme 1) and free reaction products and since accumulation of any potential covalent enzyme intermediate species E-dRSP, which would migrate on the origin of the TLC system used for the assays, was not observed, this is the rate of the slowest first-order step up to and including the chemical step of cleavage of the dGMP glycosidic bond.

Using the single turnover assay,  $k_{\text{obs}}$  for WT was determined to be  $0.062 \pm 0.005 \text{ s}^{-1}$ . The relatively close agreement between this rate and the steady-state  $k_{\text{cat}}$  for dGMP hydrolysis suggests that the chemical step of WT RCL may be rate limiting during the steady-state measurement. When Tyr13 was conservatively mutated to phenylalanine, the measured  $k_{\text{obs}}$  were markedly reduced, as indicated in Table 1, and as with WT, the value reasonably agrees with the corresponding steady-state turnover rate,  $k_{\text{cat}}$ . The significant reduction in  $k_{\text{obs}}$  parallels with the steady-state  $k_{\text{cat}}/K_{\text{M}}$ , which also reflects those steps up to and including the irreversible step, likely the initial bond cleavage event, and is as expected of residue that plays critical role during the chemical cleavage of the glycosidic bond, confirming that Tyr13 is important for dGMP hydrolysis.

**Ser87 and Ser117 Are Important for Phosphate Recognition.** On the basis of the apoenzyme structure, the residues of Ser17, Arg19, Ser87, and Ser117<sup>#</sup> were suggested to be important for recognition of the dGMP phosphate group.<sup>11</sup> The phosphate-binding role of Ser17 and Ser117<sup>#</sup> has also been implicated in the GMP-bound D69A-RCL complex structure.<sup>12</sup> In the current study, each residue was mutated with an alanine residue followed by <sup>32</sup>P assay, and the steady-state kinetic parameters are summarized in Table 1. As revealed, the mutation of Ser87 and Ser117 indeed increased the  $K_{\text{M}}$  from 89 μM of WT to 1.2 and 3.6 mM, respectively, roughly 13- and 40-fold loss in substrate binding affinity. In particular, the result of S87A closely resembles the mutational consequence of the equivalent residue Asp92 in the transferases,<sup>16</sup> which contributes to the binding of 5'-hydroxyl group in the substrate nucleoside.<sup>13</sup> The hydrolytic

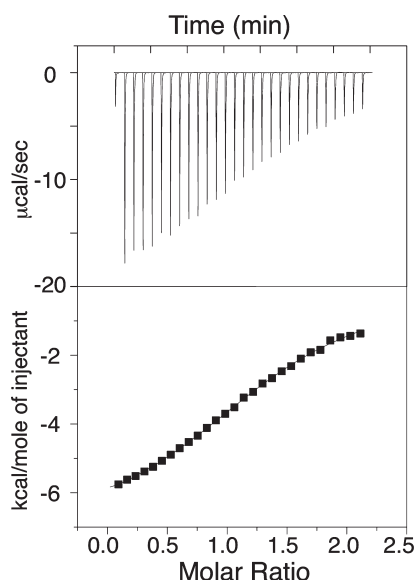


**Figure 4.** ITC profile of S87A upon titration of the inhibitor GMP. The data were best-fitted with one-site binding model.

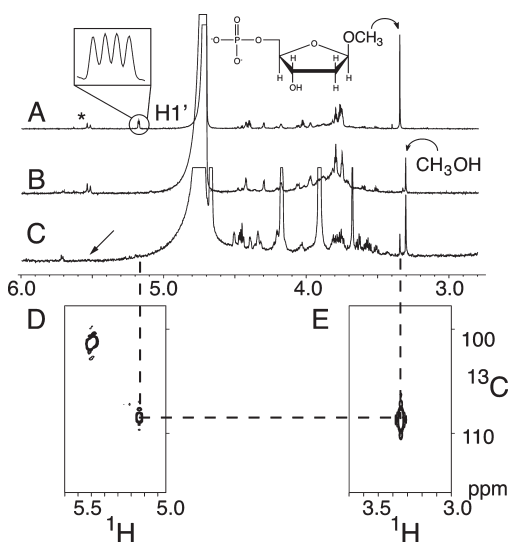


**Figure 5.** NMR studies of methanolysis of dGMP by RCL:  $^1\text{H}$  spectrum of the hydrolysis mixture of dGMP in the presence (A) and absence (B) of 20% methanol and (C) in the presence of both 20% methanol and dRSP-aldolase after 5 h reaction. (D) Selected 2D  $^1\text{H}$ – $^{13}\text{C}$  HSQC showing the  $\text{H1}'$ – $\text{C1}'$  correlation, and 2D  $^1\text{H}$ – $^{13}\text{C}$  HMBC (E) revealing three-bond  $J$  correlation between  $-\text{OCH}_3$  proton and  $\text{C1}'$  carbon. Methanol was added into (B) after RCL was heat-deactivated for the purpose of reference. The anomeric  $\text{H1}'$  signals of normal dRSP are denoted by asterisk with virtually identical carbon chemical shift in (D), and the missing  $\text{H1}'$  signal in dRSP-aldolase treated sample (C) is indicated by the arrow. The insert reveals the  $\text{H1}'$  quartets of the methylated-dRSP with two  $J$ -coupling constants expected for  $\beta$ -configuration.

activity of RCL is more significantly affected by the mutation of Ser117<sup>#</sup>, which is equivalent to Asn123 in the NDT participating in stabilizing the same 5'-hydroxyl group.<sup>13</sup> The fact that this residue is located on the fourth  $\alpha$ -helix from the neighboring subunit reinforces the view that only the dimeric form of RCL is functionally active. Comparatively, the contribution of

Ser17 and Arg19 to the phosphate binding is much smaller (Table 1).

The presence of a 2'-hydroxyl group makes GMP an inhibitor for RCL.<sup>1</sup> The binding affinities for GMP by these mutants were investigated by using isothermal titration calorimetry (ITC) (Figure 4). Consistently, binding of GMP is markedly reduced upon mutation of either Ser87 or Ser117 with >30- and 80-fold, respectively, whereas that of Ser17 or Arg19 appears to be less affected. In conclusion, both Ser87 and Ser117 are important for substrate binding likely by specifically recognizing the phosphate group of dGMP.

**RCL-Catalyzed Reaction Involves an Intermediate.** High similarity of topology and the conservation of active site residues of RCL with NDT prompted us to hypothesize a similar catalytic mechanism via formation of a reaction intermediate following the departure of nucleobase. This intermediate, if exists, can be probed by methanolysis since it may be subjected to solvent nucleophilic attack to yield a methoxy product.

When the catalytic reaction occurs in aqueous solvent, the product(s) shows two sets of peaks at  $\sim 5.5$  ppm in  $^1\text{H}$  NMR (Figure 5B). Since both of them are attached to a  $^{13}\text{C}$  atom of 101 ppm evidenced in 2D  $^1\text{H}$ – $^{13}\text{C}$  HSQC (Figure 5D) HSQC, they were assigned to  $\text{H1}'$  proton of the dRSP in two anomeric states, either as the direct product of reaction or due to an anomeric effect. In the presence of 20% methanol, extra signals were observed at 3.31 and 5.15 ppm with a peak integral ratio of 3:1 (Figure 5A). The former has a cross-peak to a  $^{13}\text{C}$  of  $\sim 56$  ppm, indicative of a methoxy moiety, whereas the latter is correlated with a  $^{13}\text{C}$  of 109 ppm, characteristic of  $\text{H1}'$  (Figure 5D). Their through-bond correlations was unambiguously established by 2D  $^1\text{H}$ – $^{13}\text{C}$  HMBC (Figure 5E), in which the methyl protons at 3.31 ppm show a strong correlation to the  $\text{C1}'$  resonance at 109 ppm. The NMR analysis thus unequivocally identified the potential product of the methanolysis reaction, 1-*O*-methyldeoxyribose 5'-monophosphate (MeO-dRSP). Furthermore, unlike dRSP, the methoxy group at  $\text{C1}'$  position prevents the mutarotation at the anomeric site, enabling us to establish the stereochemical configuration along the reaction pathway. Since the vicinal coupling constants (dd, 2.7 and 5.5 Hz) of  $\text{H1}'$  at 5.15 ppm agree extremely well with those in methyl-2'-deoxy- $\beta$ -ribofuranoside rather than the corresponding  $\alpha$ -anomer (dd, 5.3 and 1.0 Hz),<sup>24</sup> it is concluded that the  $\beta$ -configuration of dGMP is retained in the product, in accordance with a ping-pong mechanism. Next, we applied the same methanolysis experiment on E93A and Y13F mutants. In consistent with their kinetic data, Y13F but not E93A is capable of producing a methylated product with a retention of the  $\beta$ -conformation. In conclusion, the methanolysis study rules out a mechanism involving direct nucleophilic attack from an enzyme-activated water molecule<sup>19,25</sup> and strongly suggests that RCL hydrolyzes dGMP via the formation of an intermediate potentially in a manner similar to the transferases<sup>14</sup> and the retaining glycoside hydrolases.<sup>26</sup>

It is noteworthy that the formation of the methanolysis product, MeO-dRSP, is kinetically correlated with the formation of dRSP from two lines of evidence. First, during hydrolysis of 4 mM dGMP in the presence of 20% methanol, the integrated peak intensity of  $\text{H1}'$  of dRSP and that of  $\text{OCH}_3$  from MeO-dRSP increased concurrently with their ratio being relatively constant up to 20 h. Significant increase of the methylated product may be observed at the consumption of dRSP with prolonged incubation after all dGMP substrates were hydrolyzed. These observations suggest that the reversible reaction from

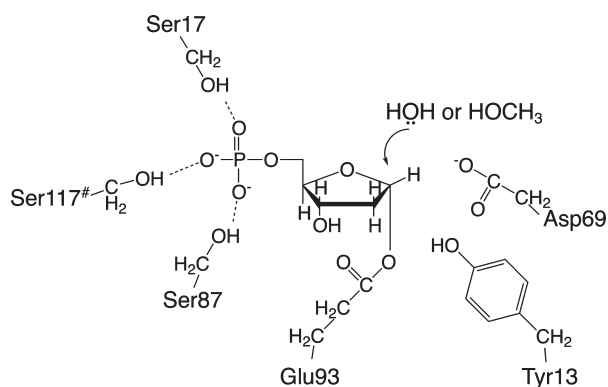


**Figure 6.** Schematic diagram summarizing the experimental results, presenting one possible intermediate with Glu93 covalently linked to the C1' of dRSP. The intermediate may be subjected to nucleophilic attack by solvent water or methanol molecules.

dRSP to the MeO-dRSP is comparatively slow and that the formation of the MeO-dRSP parallels with the formation of dRSP at the beginning of the hydrolytic reaction. Second, we performed the methanolysis reaction in the presence of dRSP-aldolase,<sup>1</sup> which can quickly consume the normal hydrolytic product dRSP and prevent it from being slowly converted to MeO-dRSP. As shown in Figure 5C, the H1' signal of dRSP is missing, whereas the intensity of the OCH<sub>3</sub> peak from the methanolysis product is comparable with the one observed in a similar reaction but in the absence of the dRSP-aldolase, suggesting that formation of MeO-dRSP is independent of dRSP. In conclusion, the methanolysis study strongly suggests the formation of a reaction intermediate along the catalytic pathway.

## DISCUSSION

RCL represents a new class of nucleotide hydrolases that catalyze the cleavage of the glycosidic bond of a nucleotide. Sequence alignment of the family members from 13 species intriguingly revealed that residues are highly conserved throughout the interfacial helices, indicating a prevalent dimerization in RCL family.<sup>11</sup> Rigorously, the dimerization step should be taken into account in the kinetic data analysis as well as in the mutational interpretation. However, the current analysis was carried out without inclusion of such a step for the following reasons. First, the majority of the mutation sites are not directly involved in the dimeric interface interactions. It is conceivable that the dissociation constant is hardly affected by these mutations. Second, most of kinetic parameters listed in Table 1 were obtained with protein concentrations above 100  $\mu$ M, at which dimer is predominant by several lines of evidence including size-exclusion chromatography.<sup>11</sup> And last, typically two protein concentrations were performed to ensure that the measured  $k_{\text{cat}}$  and  $K_{\text{m}}$  are not protein concentration dependent.

One may argue whether the dimeric active form is physiologically relevant. While this question is beyond the current scope, it is plausible that in untransformed cells RCL may exist in the inactive monomeric form with its expression at basal level, whereas in tumor cells significant upregulation by c-Myc or others may activate RCL assuming the dimeric functional form.<sup>2</sup> A similar monomer/dimer activation switch was also proposed in human cytomegalovirus protease<sup>21</sup> and the Coronavirus 3D-like protease from SARS.<sup>27</sup>

Methanolysis is a unique method in enzymatic study. For example, it has been successfully utilized to differentiate retaining glycoside hydrolases from the inverting homologues, as the ability of forming a methylglycoside product is restricted to a double-displacement mechanism involving an enzyme–sugar intermediate.<sup>25,28</sup> In this work, our methanolysis results led us to propose a mechanism as outlined in Scheme 1, including the formation of an intermediate and conservation of the sugar stereochemical conformation as observed in the methanolysis product. Given the sequence and structural similarity between RCL and the NDTs, we attempt to propose a similar covalent RCL–ribose intermediate as further depicted in Figure 6. Since E93A is incapable of forming a reaction intermediate and completely loses its hydrolytic activity, it is conceivable that Glu93 may serve as the nucleophile in the bond cleavage step reminiscent of the equivalent glutamyl residue in the transferase<sup>14</sup> and the glycosidases.<sup>26</sup> However, other forms of intermediate, such as a glycal intermediate, cannot currently be excluded. As for Tyr13, the equivalent Tyr in NDTs is dispensable for the hydrolytic activity,<sup>16</sup> and the residue was proposed to orient either the substrate at the active site or the side chain of the catalytic residue Glu93.<sup>13,15,16</sup> While the present knowledge could not rule out a similar functional role that could be assumed by this Tyr13 in RCL, this tyrosyl residue arguably has a much more profound impact on the enzyme activity considering the larger magnitude of the activity loss upon mutation.

In NDTs, hydrolysis of the ribosylated intermediate in the absence of an acceptor nucleobase was suggested to be rate limiting, and the rate was only affected by mutation of the nucleophilic glutamyl residue.<sup>16</sup> In RCL, by contrast, single turnover study suggests that the corresponding step is not the bottleneck of the reaction. In the simplest kinetic interpretation and in the absence of evidence for additional steps such as conformational changes prior to chemistry, the  $k_{\text{obs}}$  likely reflects the rate of the chemical step that leads to formation of the reaction intermediate ( $k_{\text{chem}}$  in Scheme 1). Consistent with this proposition, most of the mutant proteins exhibit decreased  $k_{\text{cat}}/K_{\text{m}}$  as shown in Table 1, reflecting that these residues affect the steps up to and including the rate-limiting irreversible glycosidic bond cleavage. This difference between NDTs and RCL may be partially attributed to the structural difference of the C-terminal tail. In case of transferases, the C-terminal carboxyl group loops back, reaching to the bottom of the active site pocket, poised to facilitate the base binding.<sup>15</sup> The flexible C-terminal tail of RCL, on the contrary, fails to make similar interaction with the base,<sup>12</sup> resulting in potential loss of the selection of base over solvent nucleophile.

Finally, RCL differs from the transferase family of proteins by possessing a phosphate binding pocket, comprising residues of Ser87, Ser117<sup>#</sup>, and possibly Ser17, as shown in Figure 6. The important role of Ser87 is further elaborated by the report on another family member—pyrimidine nucleotide hydrolase Blsm—in which the mutation of the equivalent serine to an aspartyl residue completely abolished its hydrolytic reaction.<sup>23</sup> Another important residue for the phosphate group recognition is Ser117<sup>#</sup>. Since it is located in the neighboring subunit, it could be envisioned that the substrate binding may encourage the dimer formation, a notion which may explain the smaller value of the apparent RCL dissociation constant in the presence of dGMP than the one in apo-RCL.<sup>1</sup> It was also reported in the inosine monophosphate cyclohydrolase that substrate binding may promote enzyme dimeric form.<sup>29–31</sup> Ser17 also appears to be quite important for substrate binding, as mutation of this residue



to an alanine resulted in ~10-fold decreases in  $k_{cat}/K_m$ . Interestingly, Ser17 is one of a few sites in RCL subjected to phosphorylation *in vivo*,<sup>32</sup> possibly regulating RCL's activity by reducing substrate binding.<sup>17</sup>

In summary, the current study strongly suggests that RCL not only shares sequence homology and similar tertiary fold with NDTs; functionally it also resembles NDTs but with clear distinction. Further in-depth study undoubtedly will lead to full understanding of this enzyme and thus help us design therapeutic strategy to treat RCL-related diseases.

## AUTHOR INFORMATION

### Corresponding Author

\*Tel: 614-247-5040. Fax: 614-292-6773 E-mail: wu.473@osu.edu.

### Funding Sources

This work was funded in part by NSF MCB-0719264 and NIH R21EY018423.

## ACKNOWLEDGMENT

We thank Dr. Bessman, MJ, for providing the mutT clone and the anonymous reviewers for their critical suggestions.

## ABBREVIATIONS

dGMP, deoxyguanine monophosphate; GMP, guanine monophosphate; HNBC, heteronuclear multiple bond correlation; hsqc, heteronuclear single quantum coherence; ITC, isothermal titration calorimetry; NMR, nuclear magnetic resonance; RCL, responsive to c-Myc; NDT, nucleoside deoxyribosyltransferase.

## REFERENCES

- (1) Ghiorgi, Y. K., Zeller, K. I., Dang, C. V., and Kaminski, P. A. (2007) The c-Myc target gene Rcl (C6orf108) encodes a novel enzyme, deoxynucleoside 5'-monophosphate N-glycosidase. *J. Biol. Chem.* 282, 8150–8156.
- (2) Lewis, B. C., Shim, H., Li, Q., Wu, C. S., Lee, L. A., Maity, A., and Dang, C. V. (1997) Identification of putative c-Myc-responsive genes: characterization of rcl, a novel growth-related gene. *Mol. Cell. Biol.* 17, 4967–4978.
- (3) Chan, C. P., But, P. P., and Ho, J. W. (2002) Induction of rcl, a novel growth-related gene by coptidis rhizoma in rat H4IIE cells. *Life Sci.* 70, 1691–1699.
- (4) Almon, R. R., DuBois, D. C., and Jusko, W. J. (2007) A microarray analysis of the temporal response of liver to methylprednisolone: a comparative analysis of two dosing regimens. *Endocrinology* 148, 2209–2225.
- (5) Miki, Y., Suzuki, T., Tazawa, C., Ishizuka, M., Semba, S., Gorai, I., and Sasano, H. (2005) Analysis of gene expression induced by diethylstilbestrol (DES) in human primitive Mullerian duct cells using microarray. *Cancer Lett.* 220, 197–210.
- (6) Shin, S., Bosc, D. G., Ingle, J. N., Spelsberg, T. C., and Janknecht, R. (2008) Rcl is a novel ETV1/ER81 target gene upregulated in breast tumors. *J. Cell. Biochem.* 105, 866–874.
- (7) Rhodes, D. R., Barrette, T. R., Rubin, M. A., Ghosh, D., and Chinnaiyan, A. M. (2002) Meta-analysis of microarrays: interstudy validation of gene expression profiles reveals pathway dysregulation in prostate cancer. *Cancer Res.* 62, 4427–4433.
- (8) Kim, S. Y., Herbst, A., Tworkowski, K. A., Salghetti, S. E., and Tansey, W. P. (2003) Skp2 regulates Myc protein stability and activity. *Mol. Cell* 11, 1177–1188.

- (9) Keller, U., Nilsson, J. A., Maclean, K. H., Old, J. B., and Cleveland, J. L. (2005) Nfkb 1 is dispensable for Myc-induced lymphomagenesis. *Oncogene* 24, 6231–6240.
- (10) Zeller, K. I., Jegga, A. G., Aronow, B. J., O'Donnell, K. A., and Dang, C. V. (2003) An integrated database of genes responsive to the Myc oncogenic transcription factor: identification of direct genomic targets. *Genome Biol.* 4, R69.
- (11) Doddapaneni, K., Mahler, B., Pavlovicz, R., Haushalter, A., Yuan, C., and Wu, Z. (2009) Solution structure of RCL, a novel 2'-deoxyribonucleoside 5'-monophosphate N-glycosidase. *J. Mol. Biol.* 394, 423–434.
- (12) Yang, Y., Padilla, A., Zhang, C., Labesse, G., and Kaminski, P. A. (2009) Structural characterization of the mammalian deoxynucleotide N-hydrolase Rcl and its stabilizing interactions with two inhibitors. *J. Mol. Biol.* 394, 435–447.
- (13) Armstrong, S. R., Cook, W. J., Short, S. A., and Ealick, S. E. (1996) Crystal structures of nucleoside 2-deoxyribosyltransferase in native and ligand-bound forms reveal architecture of the active site. *Structure* 4, 97–107.
- (14) Porter, D. J., Merrill, B. M., and Short, S. A. (1995) Identification of the active site nucleophile in nucleoside 2-deoxyribosyltransferase as glutamic acid 98. *J. Biol. Chem.* 270, 15551–15556.
- (15) Anand, R., Kaminski, P. A., and Ealick, S. E. (2004) Structures of purine 2'-deoxyribosyltransferase, substrate complexes, and the ribosylated enzyme intermediate at 2.0 Å resolution. *Biochemistry* 43, 2384–2393.
- (16) Short, S. A., Armstrong, S. R., Ealick, S. E., and Porter, D. J. (1996) Active site amino acids that participate in the catalytic mechanism of nucleoside 2'-deoxyribosyltransferase. *J. Biol. Chem.* 271, 4978–4987.
- (17) Dupouy, C., Zhang, C., Padilla, A., Pochet, S., and Kaminski, P. A. (2010) Probing the Active Site of the Deoxynucleotide N-Hydrolase Rcl Encoded by the Rat Gene c6orf108. *J. Biol. Chem.* 285, 41806–41814.
- (18) Versees, W., and Steyaert, J. (2003) Catalysis by nucleoside hydrolases. *Curr. Opin. Struct. Biol.* 13, 731–738.
- (19) Parkin, D. W., Horenstein, B. A., Abdulah, D. R., Estupinan, B., and Schramm, V. L. (1991) Nucleoside hydrolase from Crithidia fasciculata. Metabolic role, purification, specificity, and kinetic mechanism. *J. Biol. Chem.* 266, 20658–20665.
- (20) Bhatnagar, S. K., Bullions, L. C., and Bessman, M. J. (1991) Characterization of the mutT nucleoside triphosphatase of Escherichia coli. *J. Biol. Chem.* 266, 9050–9054.
- (21) Darke, P. L., Cole, J. L., Waxman, L., Hall, D. L., Sardana, M. K., and Kuo, L. C. (1996) Active human cytomegalovirus protease is a dimer. *J. Biol. Chem.* 271, 7445–7449.
- (22) Bax, A., and Summers, M. F. (1986) <sup>1</sup>H and <sup>13</sup>C assignments from sensitivity enhanced detection of heteronuclear multiple bond connectivity by 2D multiple quantum NMR. *J. Am. Chem. Soc.* 108, 2093–2094.
- (23) Grochowski, L. L., and Zabriske, T. M. (2006) Characterization of BlsM, a nucleotide hydrolase involved in cytosine production for the biosynthesis of blasticidin S. *ChemBioChem* 7, 957–964.
- (24) Raap, J., Vanboom, J. H., Vanlieshout, H. C., and Haasnoot, C. A. G. (1988) Conformations of Methyl 2'-Deoxy-Alpha-D-Ribofuranoside and Methyl 2'-Deoxy-Beta-D-Ribofuranoside - a Proton Magnetic-Resonance Spectroscopy and Molecular Mechanics Study. *J. Am. Chem. Soc.* 110, 2736–2743.
- (25) Shallom, D., Belakhov, V., Solomon, D., Shoham, G., Baasov, T., and Shoham, Y. (2002) Detailed kinetic analysis and identification of the nucleophile in alpha-L-arabinofuranosidase from Geobacillus stearothermophilus T-6, a family 51 glycoside hydrolase. *J. Biol. Chem.* 277, 43667–43673.
- (26) McCarter, J. D., and Withers, S. G. (1994) Mechanisms of enzymatic glycoside hydrolysis. *Curr. Opin. Struct. Biol.* 4, 885–892.
- (27) Shi, J., Sivaraman, J., and Song, J. (2008) Mechanism for controlling the dimer-monomer switch and coupling dimerization to catalysis of the severe acute respiratory syndrome coronavirus 3C-like protease. *J. Virol.* 82, 4620–4629.

- (28) Pitson, S. M., Voragen, A. G., and Beldman, G. (1996) Stereochemical course of hydrolysis catalyzed by arabinofuranosyl hydrolases. *FEBS Lett.* 398, 7–11.
- (29) Xu, L., Chong, Y., Hwang, I., D'Onofrio, A., Amore, K., Beardsley, G. P., Li, C., Olson, A. J., Boger, D. L., and Wilson, I. A. (2007) Structure-based design, synthesis, evaluation, and crystal structures of transition state analogue inhibitors of inosine monophosphate cyclohydrolase. *J. Biol. Chem.* 282, 13033–13046.
- (30) Vergis, J. M., and Beardsley, G. P. (2004) Catalytic mechanism of the cyclohydrolase activity of human aminoimidazole carboxamide ribonucleotide formyltransferase/inosine monophosphate cyclohydrolase. *Biochemistry* 43, 1184–1192.
- (31) Bullock, K. G., Beardsley, G. P., and Anderson, K. S. (2002) The kinetic mechanism of the human bifunctional enzyme ATIC (5-amino-4-imidazolecarboxamide ribonucleotide transformylase/inosine 5'-monophosphate cyclohydrolase). A surprising lack of substrate channeling. *J. Biol. Chem.* 277, 22168–22174.
- (32) Olsen, J. V., Blagoev, B., Gnäd, F., Macek, B., Kumar, C., Mortensen, P., and Mann, M. (2006) Global, in vivo, and site-specific phosphorylation dynamics in signaling networks. *Cell* 127, 635–648.